  Bull. Chem. Soc. Jpn., 56, 3065—3072 (1983)

Double Potential Step Chronoamperometry for Reversible Follow-up Chemical Reactions. Application to the Aquation Kinetics of Bis(ethylenediaminemonoacetato)cobalt(II)

Takeo OHSAKA, Tadashi SOTOMURA,†,†† Hiroaki MATSUDA,† and Noboru OYAMA*

Department of Applied Chemistry for Resources, Tokyo University of Agriculture and Technology, Koganei, Tokyo 184

†*Department of Electronic Chemistry, Graduate School at Nagatsuta, Tokyo Institute of Technology, Nagatsuta, Midori-ku, Yokohama 227*

(Received April 30, 1983)

A theory of double potential step chronoamperometry (DPSCA) is developed for the reversible follow-up reactions represented as $Ox+ne \rightleftarrows Red$, $Red \underset{kK}{\overset{k}{\rightleftarrows}} Z$, where k and K are the rate and the equilibrium constants of the follow-up chemical reaction, respectively. DPSCA is applied to investigate the kinetics of aquation reaction of $[Co(edma)_2]^0$ (edma: ethylenediamine-*N*-acetate), which is produced by electrolytic reduction of $[Co(edma)_2]^+$ in the range of pH 1.5 to 10.5. At pH<4.5, the aquation reaction of $[Co(edma)_2]^0$ is irreversible. The rate of aquation reaction is accelerated by hydrogen ions and approaches an upper limiting value (2.1×10^3 s^{-1}). At pH> 4.5, on the other hand, the hydrogen ions do not substantially contribute to the aquation and thus the rate approaches a lower limiting value (4.7×10^2 s^{-1}), which is in good agreement with that obtained in neutral region (4.5< pH<7), where the reverse (complex formation) reaction must be taken into consideration. Above pH 7, the $[Co(edma)_2]^0$ species exists as main species in the solution and thus the kinetic behavior of the aquation is not observed. It is demonstrated that DPSCA is a useful method for kinetic studies of the dissociation-association reactions of labile complexes.

The double potential step (DPS) chronoamperometry (CA) and the DPS chronocoulometry (CC) are well-developed techniques for studying the kinetics of homogeneous chemical reactions of the species, which may be produced by charge transfer reactions. Schwarz and Shain[1] first presented the DPSCA to determine the rate constant of the benzidine rearrangement reaction and showed that this technique has a high potentiality for the determination of rate constants of follow-up chemical reactions. Christie[2] modified the technique originally devised by Schwarz and Shain by recording the charge *vs.* time variations instead of the current *vs.* time curves, and this modified technique is usually referred to as DPSCC. Since then, various authors have reported several modifications of these techniques[3-9] as well as their application to practical problems.[10-20] However, almost all treatments reported up to date are restricted to completely irreversible follow-up reactions. The recent paper of Hanafey *et al.*[9] is only one exceptional one, in which they reported the explicit finite difference simulation of DPS current, charge and absorbance responces for 22 two-parameter electrochemical mechanisms, including the second-order kinetics.

Recently, we have attempted an application of DPSCA to the kinetics of aquation reactions of labile complexes which may be produced by charge transfer reactions of the corresponding inert complexes. In this case, if it is desired to perform measurements in a wide range of free ligand concentrations or of pH, the effects of the reverse (complex formation) reactions should be taken into consideration. Then, the follow-up reactions must be regarded as reversible. In the present paper, we shall develope a theory of DPSCA for reversible follow-up reactions in an analytical way and apply it to determining the rate constant of aquation reaction of bis(ethylenediaminemonoacetato)cobalt(II), which is produced by electrolytic reduction of bis(ethylenediaminemonoacetato)cobalt(III) (corresponding inert complex species).

Theoretical

Consider the electrode reaction followed by a first-order chemical reaction, which is symbolically represented by

$$Ox + ne \rightleftarrows Red, \quad Red \underset{kK}{\overset{k}{\rightleftarrows}} Z,$$

where k and K are the rate and the equilibrium constants of the follow-up chemical reaction, respectively. The plane boundary value problem for the diffusion processes corresponding to the above mechanism can be solved by utilizing the method of Laplace transformation under the assumption that the diffusion coefficients of Red and Z have the common value.[21] Thus, the concentration of Ox and Red at the electrode surface, C_O^s and C_R^s, can be expressed as

$$C_O^s = C_O^\circ - \frac{1}{\sqrt{D_O\pi}}\int_0^t \frac{[i(u)/nFA]}{\sqrt{t-u}}du, \tag{1}$$

$$C_R^s = \frac{1}{(1+K)\sqrt{D\pi}}\int_0^t \frac{K+\exp[-\rho(t-u)]}{\sqrt{t-u}}[i(u)/nFA]du, \tag{2}$$

with

$$\rho = k(1+K), \tag{3}$$

where C_O° denotes the bulk concentration of Ox; the bulk concentrations of Red and Z are assumed to be equal to zero; D_O is the diffusion coefficient of Ox; D is the common diffusion coefficient of Red and Z; $i(t)$ denotes the current intensity; A is the surface area of the electrode; t is the lapse of the time after the beginning of the electrolysis.

The electrolysis condition of DPSCA is as follows:

†† Present address: Matsushita Electric Industrial Co., Ltd., 1006, Kadoma, Kadoma, Osaka 571.

the potential is stepped from some initial value, where no current flows, to a value which causes the electrode reaction product, Red, to be generated at a diffusion-controlled rate. After a given generation time, τ, the potential is returned to the initial value, where the electrode reaction is reversed, consuming Red at a diffusion-controlled rate. Thus, the electrolysis condition can be expressed by

$$0 < t < \tau : C_O^S = 0, \tag{4}$$

$$\tau < t : C_R^S = 0, \tag{5}$$

For $0<t<\tau$, inserting Eq. 1 into Eq. 4 and solving the resultant Abel integral equation yields immediately the cathodic limiting diffusion current, i_c:

$$i_c = nFA\, C_O^\circ \sqrt{D_O}/\sqrt{\pi t}. \tag{6}$$

For $t>\tau$, on the other hand, substituting Eq. 2 into Eq. 5 and noting that the current intensity during the first potential pulse ($0<t<\tau$) is given by Eq. 6, we obtain after some rearrangements

$$\int_\tau^t \frac{K+\exp[-\rho(t-u)]}{\sqrt{t-u}} \left\{ \frac{-i_a(u)}{nFA} + \frac{C_O^\circ \sqrt{D_O}}{\sqrt{\pi u}} \right\} du = \frac{C_O^\circ \sqrt{D_O}}{\sqrt{\pi}} \int_0^t \frac{K+\exp[-\rho(t-u)]}{\sqrt{u(t-u)}} du, \tag{7}$$

where i_a denotes the anodic current to be measured for $t>\tau$. Here, it is convenient to introduce the dimensionless variable:

$$\xi = (t-\tau)/\tau, \tag{8}$$

which denotes the portion of the lapse of time after the beginning of the second potential pulse to the switching time τ. Further, we introduce new integral variables: $u=\tau(1+v)$ and $u=\tau(1+\xi)(1-v)$ into the left- and right-hand sides of Eq. 7, respectively. Then we obtain after evaluating the definite integral on the right-hand side of the resulting equation[22]

$$\int_0^\xi \frac{K+\exp[-\rho\tau(\xi-v)]}{\sqrt{v(\xi-v)}} \Psi(v) dv = \pi \left\{ K+\exp[-(\rho\tau/2)(1+\xi)] I_0\left(\frac{\rho\tau}{2}[1+\xi] \right) \right\}, \tag{9}$$

with

$$\Psi(v) = (-i_a/i_c) + \sqrt{\xi/(1+\xi)}, \tag{10}$$

where I_0 is the zero-order modified Bessel function of the first kind. $(-i_a/i_c)$ denotes the ratio of the anodic current measured at a given time t during the second pulse to the cathodic current measured at $(t-\tau)$ during the first pulse, and will be used for constructing the working curves, following the suggestion of Schwarz and Shain.[1] Since Eq. 9 is the Volterra integral equation of the first kind with respect to $\Psi(\xi)$, its analytical solution may be obtained in a closed form by utilizing the method of Laplace transformation. However, when practically constructing the working curves by using the analytical solution, it is necessary to evaluate numerically the definite integral. Such a numerical method is described in Appendix. Numerical calculations were performed for various combinations of the values of K and $k\tau$ by means of a digital computer FACOM M-160, and the values of $\Psi(\xi)$ were obtained as functions of ξ. Then, for a given constant value of ξ, say $\xi=1$, the working curves, *i.e.*, $(-i_a/i_c)$ *vs.* $k\tau$ plots, were drawn for a series of values of K. As examples, such working curves constructed for $\xi=1$ are shown for a series of values of K in Fig. 1. Of course, the curve for $K=0$ is in agreement with that of Schwarz and Shain.[1] As can be seen from Fig. 1, when the parameter $k\tau$ is increased, the working curves are at first decreased and then, after passing through the corresponding minima, they are increased. This behavior is understandable in view of the fact that Red may be reproduced from Z by the reverse reaction during the second pulse. Thus, there arises a problem that one measured value of $(-i_a/i_c)$ corresponds to the two values of $k\tau$. This problem may simply be solved by examining whether $(-i_a/i_c)$ is decreased or increased when the switching time τ is slightly increased.

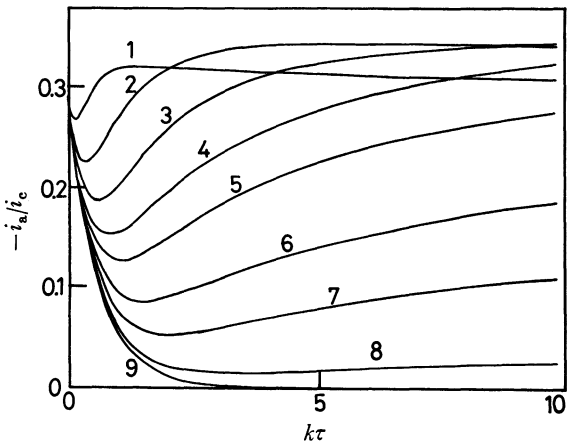

Fig. 1. Typical working curves for a series of values of K at $\xi=1$.
K: (1) 3; (2) 1; (3) 0.5; (4) 0.3; (5) 0.2; (6) 0.1; (7) 0.05; (8) 0.01; and (9) 0.

Experimental

Reagents. *Trans*-bis(ethylenediaminemonoacetato)cobalt(III) chloride dihydrate, *trans*-$[Co(edma)_2]Cl \cdot 2H_2O$, and ethylenediaminemonoacetic acid dihydrochloride dihydrate, $Hedma \cdot 2HCl \cdot 2H_2O$, were prepared and purified by the method of Fujii *et al.*,[23] where edma$^-$ is an abbreviation of $H_2NCH_2CH_2NHCH_2COO^-$. Sodium acetate and disodium hydrogen phosphate were purified by recrystallizing twice from water. All other chemicals used were prepared and purified by the methods described previously.[24]

Cell and Electrodes. The electrolytic cell used was all-glass six neck vessel of the same type as described previously,[25] which was equipped with various electrodes, argon gas inlet and outlet, and two burets. The electrode assembly consisted of a dropping mercury working electrode (DME), a saturated calomel reference electrode (SCE) and a mercury pool auxiliary electrode (AE), the latter being placed at the bottom of the cell. The characteristics of DME used were: drop time = 7.9 s and flow rate of mercury = 1.45 mg s^{-1} in 1.0 M (1 M = 1 mol dm^{-3}) $NaClO_4$ solution at 45 cm of the height of mercury head with no applied potential. The SCE was connected to the cell throught a junction salt bridge containing sodium chloride solution. A glass electrode (Beckman No. 40495) and a Ag–AgCl reference electrode were used for pH measurements of the test solutions.

Instrumentation. The pulse experiments were performed

on the solid state instrument constructed from readily available components, which consisted of a drop fall detector, timing control logic circuitry, a pulse generator and a potentiostat. A spike-like pulse, generated at the moment of drop detachment from the capillary tip, was employed as a trigger signal for the timing controlling pulse train.[26] When the spike was detected, the AE was disconnected from the potentiostat by means of a FET switch. The measuring device was a Nicolet 1090A Explorer digital oscilloscope. The current responces were monitored and stored on it and then the enlarged current-time curves were displayed on an X-Y recorder (Riken-Denshi Model F-42CP). No IR compensation was employed.

The polarograph used for preliminary experiments was the same as described previously.[24] The pH measurements were performed on an Orion Research Model 801 digital pH/mV meter.

Procedures. All measurements were performed in a paraffin oil thermostat at 25.0±0.1 °C. Two kinds of the solution composition were used: 1.0 mM *trans*-$[Co(edma)_2]^+$, 20 and 50 mM Hedma, and 1.0 M $NaClO_4$. No buffer was added in the pH ranges 1.0—3.5 and 6.5—10.0, because the ligand present in a large excess was expected to have a sufficiently large buffer capacity in these pH ranges. In the pH range 3.5—6.5, the acetate (for pH 3.5—5.5) and phosphate (for pH 5.5—6.5) buffers were used at the concentration of 50 mM. The pH values of the test solutions were changed and measured following the procedure described previously.[27] Deaeration of the solution was accomplished with pure argon gas by bubbling through the solution for 1 h before each run and with a steady flow maintained over the solution during measurements.

The potential applied to the working electrode was a single square pulse with an amplitude of 0.55 V and this pulse was applied at the moment when the mercury drop sufficiently grew, *i.e.*, 4—5 s after the beginning of the drop growth. The initial d.c. level E_i was selected from the behavior of d.c. polarographic reduction waves of *trans*-$[Co(edma)_2]^+$ as follows: $E_i=-0.05$ *V vs.* SCE for pH 1—6, $E_i=-0.10$ *V vs.* SCE for pH 6—8 and $E_i=-0.20$ *V* vs. SCE for pH 8—10. In acidic solutions the applied potentials always fell in the diffusion-controlled limiting current region for each depolarizer species. However, in the alkaline region, the foot of the mercury desolution wave slightly overlapped with the reduction wave of $[Co(edma)_2]^+$ species. Thus, data obtained in alkaline solutions may be less reliable, although several trials for selection of E_i were performed and a blank correction was made using current-time curves measured in solutions containing no $[Co(edma)_2]^+$ species.

Results and Discussion

The electrode reaction of Co(III)/Co(II)–edma system may be formally expressed by Scheme 1, where, $(k_1)_{app}$ and $(k_2)_{app}$ denote the apparent rate constants of the step-wise aquation processes, respectively.

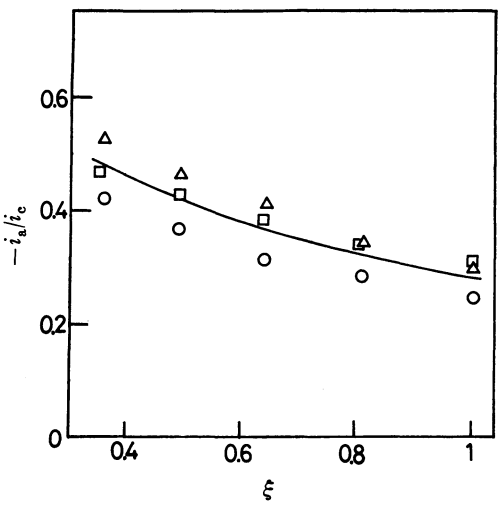

Fig. 2. Typical plots of the current ratio $(-i_a/i_c)$ *vs.* ξ under the diffusion-controlled conditions.
Concentration of *trans*-$[Co(edma)_2]^+=1.0$ mM. Total concentration of Hedma=20 mM. (□): pH 7.38, (○): pH 8.75, (△): pH 10.66. Solid line represents the theoretical curve calculated by Eq. 11.

β_{101} and β_{102} are the overall formation constants of $[Co(edma)]^+$ and $[Co(edma)_2]^0$ species, respectively, the values of which were determined previously[27] as follows: $\log \beta_{101}=7.51$ and $\log \beta_{102}=14.05$.

First, consider the reaction in the alkaline region higher than pH 7. In this pH region, $[Co(edma)_2]^0$ species is stable for the ligand concentrations of 20—50 mM and thus the aquation reaction does not occur. Therefore, the anodic-cathodic current ratio, $(-i_a/i_c)$, must satisfy the following equation for the diffusion-controlled conditions:[1]

$$(-i_a/i_c) = 1 - [\xi/(1+\xi)]^{1/2}, \qquad (11)$$

where ξ is defined by Eq. 8. Some typical results of $(-i_a/i_c)$ *vs.* ξ plot for several pH values are shown in Fig. 2, where the points are the experimental values, and the solid line represents the theoretical behavior calculated by Eq. 11. The results show that the anodic currents are essentially controlled by diffusion of $[Co(edma)_2]^0$ to the electrode surface. Slight deviations of $(-i_a/i_c)$ from theory could be attributed to the overlapping of the mercury desolution current with the anodic current of $[Co(edma)_2]^0$.

Next, the reaction in the acidic region lower than pH 4.5 will be examined. In this acidic region, the first step aquation process becomes irreversible, because the rate of the corresponding reverse process may be neglected, as can be proved from the concentrations of $[Co(edma)]^+$ and $edma^-$ calculated by the use of the

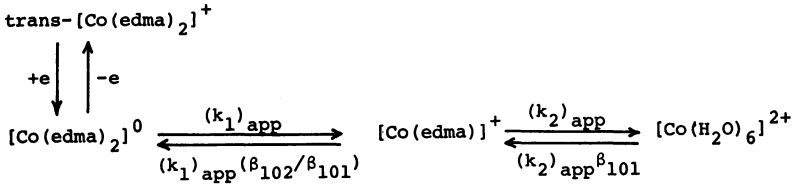

Scheme 1.

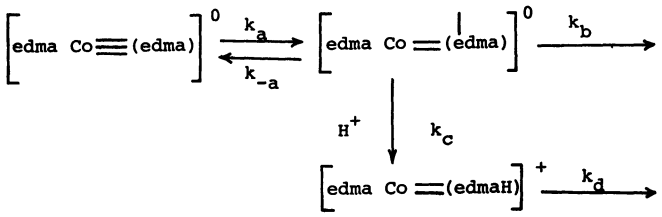

Scheme 2.

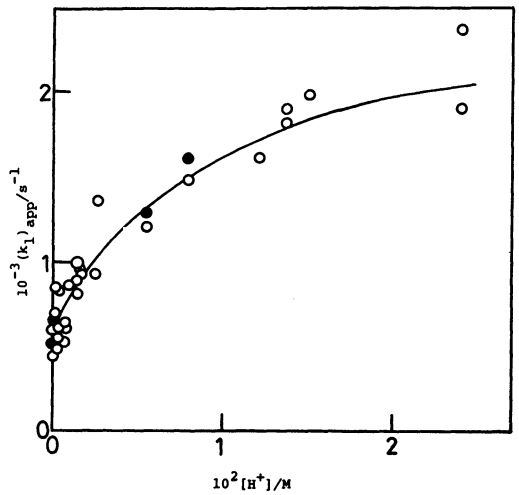

Fig. 3. Dependence of the apparent rate constant of the aquation reaction of $[Co(edma)_2]^0$ upon the concentration of hydrogen ion.
$[Co(edma)_2]^0$ was produced by the electrolytic reduction of 1.0 mM *trans*-$[Co(edma)_2]^+$ in 1.0 M $NaClO_4$ solutions containing 20 mM Hedma (open circle) or 50 mM Hedma (solid circle). The solid curve indicates the values of $(k_1)_{app}$ calculated by the use of Eq. 12 with the values of k_a, k_b/k_{-a}, and k_c/k_{-a} obtained.

formation constants of complex species and the protonation constants of edma$^-$, $\log \beta_{011}=9.97$, $\log \beta_{021}=16.71$, and $\log \beta_{031}=18.76$.[27] Therefore, analysis of the current-time curves was made by using the working curves with $K=0$ (*e.g.*, see curve 9 in Fig. 1.). The values of $(k_1)_{app}$ thus obtained for various pH values are shown in dependence of the hydrogen ion concentration, $[H^+]$, in Fig. 3. We see that the apparent rate constant greatly increases with an increase in $[H^+]$, indicating that the first aquation step is accelerated by the presence of hydrogen ion. A possible mechanism for such an acid-catalyzed dissociation of multidentate ligands may be expressed by Scheme 2, where it is assumed that the protonation of the intermediate containing bidentated edma$^-$ is irreversible, because of the fact that no evidence for the presence of protonated species was observed in potentiometric titrations.[27] Similar schemes were previously proposed for the dissociation of nickel(II),[28] iron(II),[29,30] and cobalt(II)[31–35] complexes with polyamines such as ethylenediamine (en), diethylenetriamine (dien), triethylenetetraamine (trien), 2,2′-bipyridine (bpy), 2,2′ : 6′,2″-terpyridine (terp) and 1,10-phenanthroline (phen), and the 2,4-pentanedionate complexes[36] of chromium(II), cobalt(II), and ruthenium(II). According to Sheme 2 and considering stationary-state kinetics for

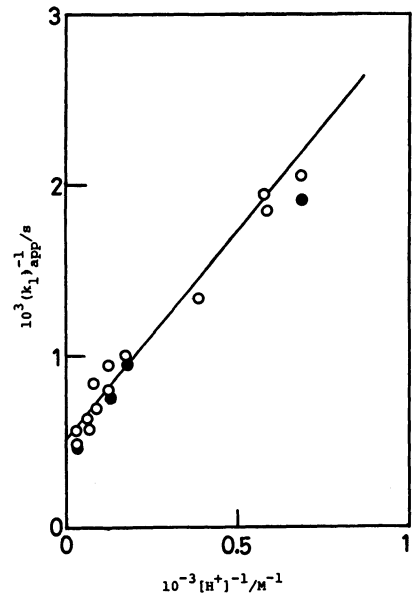

Fig. 4. Plot of $1/(k_1)_{app}$ *vs.* $1/[H^+]$.
The experimental conditions and the symbols used are the same as those in Fig. 3.

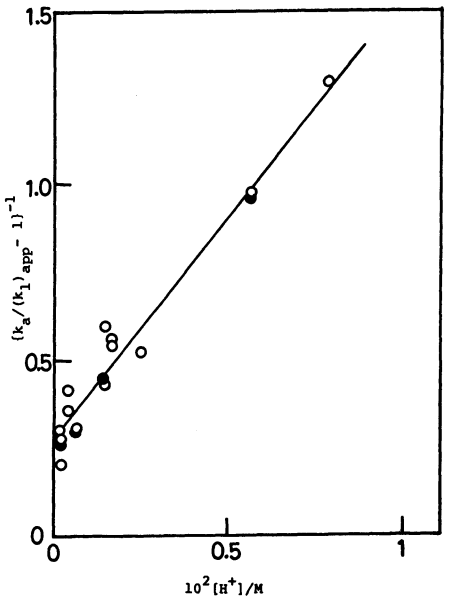

Fig. 5. Plot of $1/\{(k_a/(k_1)_{app})-1\}$ *vs.* $[H^+]$.
The experimental conditions and the symbols used are the same as those in Fig. 3.

unprotonated bidentated species, $(k_1)_{app}$ will be given by

$$(k_1)_{app}=\frac{k_a(k_b+k_c[H^+])}{k_{-a}+k_b+k_c[H^+]}. \quad (12)$$

Equation 12 can be rearranged to

$$\frac{1}{(k_1)_{app}}=\frac{1}{k_a}+\frac{k_{-a}}{k_a(k_b+k_c[H^+])}. \quad (13)$$

At sufficiently low pH where $k_b \ll k_c[H^+]$, a plot of $1/(k_1)_{app}$ *vs.* $1/[H^+]$ is linear, and k_a is derived by extrapolation to $1/[H^+]\rightarrow 0$. The graph for the first step dissociation of $[Co(edma)_2]^0$ is shown in Fig. 4. The corresponding values of the rate constants derived from the intercept and the slope are

$$k_a = 2.1 \times 10^3\ s^{-1}$$
$$(k_c/k_{-a}) = 1.9 \times 10^2.$$

Further rearrangement of Eq. 12 yields

$$1/[\{k_a/(k_1)_{app}\} - 1] = (k_b/k_{-a}) + (k_c/k_{-a})[H^+]. \quad (14)$$

Figure 5 shows the plots of $1/[\{k_a/(k_1)_{app}\} - 1]$ *vs.* $[H^+]$, which is linear as expected from Eq. 14. The intercept and the slope give the following values for the corresponding rate constants:

$$(k_b/k_{-a}) = 2.9 \times 10^{-1}$$
$$(k_c/k_{-a}) = 1.4 \times 10^2.$$

Two values of (k_c/k_{-a}) obtained from the two different plots are in good agreement with each other. To summarize briefly, the rate constant of the first step dissociation of $[Co(edma)_2]^0$ approaches to a limiting value ($2.1 \times 10^3\ s^{-1}$) for pH<1.3, in which the first bond rupture is the rate determining step for the dissociation and the hydrogen ion acts as an effective scavenger for the detached bond of bidentated edma. On the other hand, the rate constant is reduced to another limiting value ($4.7 \times 10^2\ s^{-1}$) for pH<4.3, in which the hydrogen ion does not participate directly in the dissociation process. We can calculate $(k_1)_{app}$ at various concentrations of hydrogen ion by the use of Eq. 12 with the values of k_a, k_b/k_{-a}, and k_c/k_{-a} obtained. The calculated values (solid curve in Fig. 3) are in agreement with the measured ones.

Two mechanisms are possible, depending on whether the first bond rupture occurs on the Co–N bond of a primary amino group or on the Co–O bond of carboxyl group, where the rupture of Co–N bond of secondary amino group is ruled out taking into account the steric factors. If the first bond rupture occurs on the Co–N bond of a primary amino group, the dissociation reaction proceeds through "glycinate intermediate".[37,38] On the other hand, if the Co–O bond of carboxyl group ruptures first, the subsequent dissociation reaction proceeds *via* "ethylenediamine intermediate."[37,38] The both possible reaction paths for the first step of the dissociation of $[Co(edma)_2]^0$ complex produced by the electrochemical reduction of the corresponding cobalt(III) complex can be expressed by Scheme 3, where $edma^-$ and $N\text{–}N\text{–}O^-$ stand for $NH_2\text{–}CH_2\text{–}CH_2\text{–}NH\text{–}COO^-$ and Hedma denotes the protonated $edma^-$.

As being obtained above, the rate constant of the first bond rupture corresponding to $k_{a'}$ or $k_{a''}$ is $2.1 \times 10^3\ s^{-1}$. This value is almost equal to those of the corresponding first bond rupture of $[Co(en)_2]^{2+}$ and $[Co(trien)]^{2+}$ (1.4×10^3 and 2.1×10^3, respectively).[31] Each of these three cobalt(II) complexes has four nitrogen atoms as a donating atom. Further, the rate constants of the first bond rupture of cobalt(II) complexes with $edma^-$ or such aliphatic polyamines as en, dien and trien increase in the order:[31] $[Co(en)]^{2+} < [Co(dien)]^{2+} < [Co(en)_2]^{2+} \approx [Co(trien)]^{2+} \approx [Co(edma)_2]^0 < [Co(en)_3]^{2+} \approx [Co(dien)_2]^{2+}$. It is likely that in the dissociation of cobalt(II) complexes with aliphatic polyamines and polyamine-*N*-carboxylates the rate constant of the first bond rupture increases with an increase in the number of nitrogen donor atoms. From the fact that the rate constant of the first bond rupture for $[Co(edma)_2]^0$ is almost equal to those for $[Co(trien)]^{2+}$ and $[Co(en)_2]^{2+}$, it seems reasonable that the first bond rupture occurs on the Co–N bond of a primary amino group.

The ratio k_c/k_{-a} ($(1.7 \pm 0.3) \times 10^2$) for $[Co(edma)_2]^0$ is almost equal to those for $[Co(trien)]^{2+}$ and $[Co(en)_2]^{2+}$ (3.6×10^2 and 1.6×10^2, respectively).[31] This means that for these cobalt(II) complexes the hydrolysis involving protonation is much faster than the re-

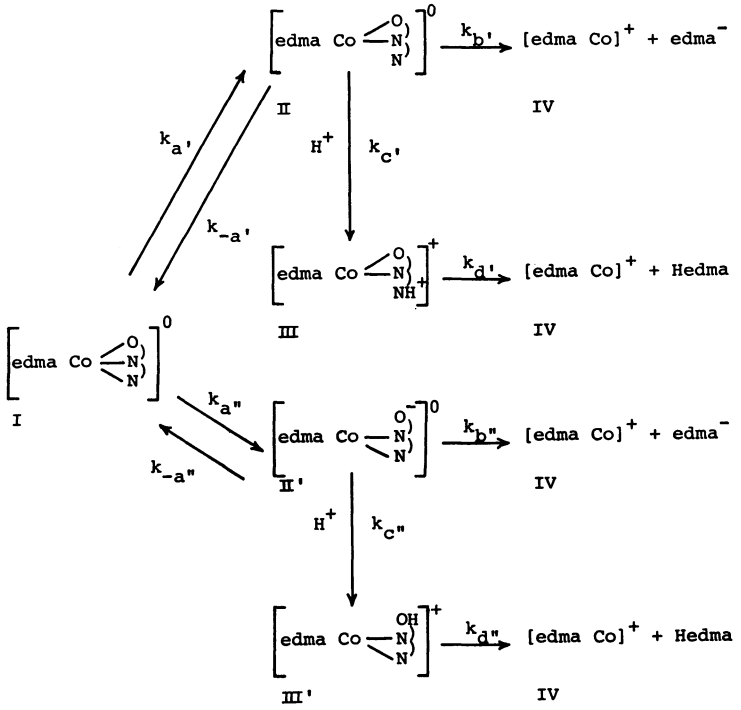

Scheme 3.

formation of the chelate ring and further for the $[Co(edma)_2]^0$ complex the protonation of an uncoordinated ligand can occur with the same easiness as those in the $[Co(en)_2]^{2+}$ and $[Co(trien)]^{2+}$ complexes.

The ratio k_b/k_{-a} is a measure of the probability for complete dissociation of a ligand once the first bond rupture occurred. The value (2.9×10^{-1}) of k_b/k_{-a} for $[Co(edma)_2]^0$ is about forty times larger than those (7.9×10^{-3})[31] for $[Co(en)_2]^{2+}$ and $[Co(trien)]^{2+}$. This may be due to the difference between the type of the bond of the still-bound ligand after the first bond rupture in the $[Co(edma)_2]^0$ dissociation and that for $[Co(en)_2]^{2+}$ and $[Co(trien)]^{2+}$. In the former the still-bound ligand has a possibility to make "glycinate intermediate" (II) and/or "ethylenediamine intermediate" (II'), while in the latter the formation of "ethylenediamine intermediate"[31] can be only expected. The processes II→IV and II'→IV shown in Scheme 3 may be considered to be similar to the first detachment processes of glycine (gly) and ethylenediamine (en) from the cobalt(II) complexes with gly and en, respectively. The rate constant of the first step of the dissociation of the $[Co(gly)_3]^-$ is by *ca.* 10 times larger than that of the $[Co(en)_3]^{2+}$.[36,39-41] Similarly, the dissociation of the nickel(II)–glycine complexes is faster than that of the corresponding ethylenediamine complexes.[42] Thus, the large difference between the value of k_b/k_{-a} for $[Co(edma)_2]^0$ and those for $[Co(en)_2]^{2+}$ and $[Co(trien)]^{2+}$ seems to eliminate the possibility of an ethylenediamine reaction mechanism in the $[Co(edma)_2]^0$ dissociation. This finding is contrary to the observation of Kodama *et al.*[37,38] obtained in their kinetic study of the substitution reactions of nickel(II)–edma$^-$ complex with diethylenetriamine-*N*, *N*,*N'*,*N''*,*N''*-pentaacetic acid (DTPA). The substitution reaction of nickel(II)–edma$^-$ complex with DTPA proceeds through "ethylenediamine intermediates."

Lastly, consider the reaction in the near neutral region of pH values from 4.5 to 7. In this pH region, the $[Co(edma)_2]^0$, $[Co(edma)]^+$, and $[Co(H_2O)_6]^{2+}$ species coexist in the solution, as can be seen from the concentration distributions calculated by the use of the formation constants of the $[Co(edma)_2]^0$ and $[Co(edma)]^+$ species and the protonation constants of edma$^-$.[27] Then the effects of the reverse (complex formation) reactions should be taken into consideration. It has been well known[41-46] that the rate constant of the first detachment step of the ligand (*i.e.*, dissociation reaction) of the labile complexes is larger than those of the subsequent steps. Thus, we assumed that the second step process $[Co(edma)]^+ \rightleftarrows [Co(H_2O)_6]^{2+}$ dose not proceed substantially compared with the first step process $[Co(edma)_2]^0 \rightleftarrows [Co(edma)]^+$ within the time scale of DPSCA. Further, the experiments were mainly conducted under the experimental conditions where $[Co(H_2O)_6]^{2+}$ ion is scarcely present in the solution. The second step process was thus ignored in examining the mechanism of overall aquation reaction of $[Co(edma)_2]^0$. Furthermore, the reaction path through the protonation of the amino group, which is the main path of the dissociation in an acidic solution, can be neglected, since the ratio of $k_c[H^+]$ to k_b which

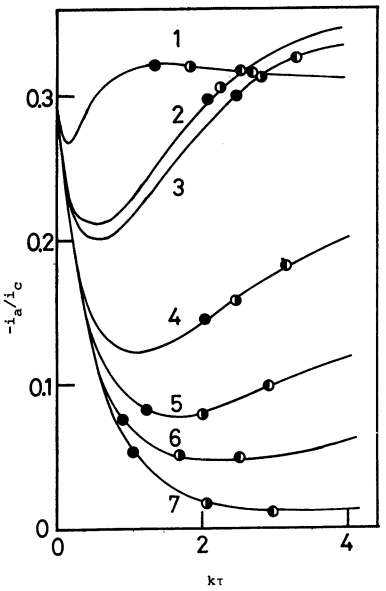

Fig. 6. Dependence of the measured values of the current ratio $(-i_a/i_c)$ on $k\tau$ for various values of K at $\xi=1$.
(●): $\tau=3.0$ ms, (◑): $\tau=4.7$ ms, (◐): $\tau=6.5$ ms.
(1): $K=3.00$, [Hedma]=20.0 mM, pH 6.22; (2): $K=0.592$, [Hedma]=20.0 mM, pH 5.84; (3): $K=0.541$, [Hedma]=15.7 mM, pH 5.90; (4): $K=0.173$, [Hedma]=60.9 mM, pH 5.32; (5): $K=0.110$, [Hedma]=40.5 mM, pH 5.30; (6): $K=0.048$, [Hedma]=20.0 mM, pH 5.20; (7): $K=0.05$, [Hedma]=14.0 mM, pH 5.00. In all cases, the concentration of *trans*-$[Co(edma)_2]^+$ is 1.0 mM. Solid lines represent the theoretical curves for various values of K which correspond to the solution compositions ((1)—(7)).

can be estimated by using the values of k_b/k_{-a} and k_c/k_{-a} obtained above is sufficiently small at pH>*ca.* 5. According to the reaction scheme (Scheme 1), the apparent rate constant, $(k)_{app}$, and the equilibrium constant, K, can be expressed by $(k_1)_{app}$ and $l(\beta_{102}/\beta_{101})$, respectively, in which l is the concentration of free edma$^-$. In Fig. 6 the experimental values of the ratio $(-i_a/i_c)$ are shown as a function of the product of the rate of the follow-up chemical reaction (k) and the switching time (τ) at various analytical concentrations of Hedma and pH's. The value of $(k_1)_{app}$ was independent of the analytical concentrations of Hedma and pH's within the experimental error, as can be expected from the above mentions. The value of $(k_1)_{app}$ was estimated to be $(4.1\pm0.6)\times10^2\ s^{-1}$, which is almost equal to the value $(4.7\times10^2\ s^{-1})$ obtained in the acidic region (pH<4.5).

The results may be summarized as follows: The mechanism of the aquation of the $[Co(edma)_2]^0$ can be described by Scheme 1 in the range of pH 1.5 to 10.6. At pH<4.5, the process of the detachment of the first edma$^-$ from the $[Co(edma)_2]^0$ is irreversible and the rate of this process is accelerated by hydrogen ions (Scheme 2). The first step of the dissociation of the $[Co(edma)_2]^0$ is the bond rupture of the Co–N bond of a primary amino group and the dissociation reaction proceeds through "glycinate intermediate" (see Scheme 3). In the region of further lower pH (pH<1), the

rate of the dissociation approaches an upper limiting value ($2.1\times10^3\ s^{-1}$). At pH>4.5, on the other hand, the hydrogen ions do not substantially contribute to the aquation and thus the rate approaches a lower limiting value ($4.7\times10^2\ s^{-1}$), which is in good agreement with that obtained in neutral region (4.5<pH<7), where the reverse (complex formation) reaction must be also taken into consideration. Above pH 7, the $[Co(edma)_2]^0$ species exists as main species in the solution and thus the kinetic behavior of the aquation is not observed.

Appendix

If we make the following substitution:

$$\eta = \sqrt{v}, \tag{A-1}$$

$$\sigma = \sqrt{\xi}. \tag{A-2}$$

Eq. 10 can be converted into the following equation;

$$2\int_0^{\sigma} \frac{K+\exp[-\rho\tau(\sigma^2-\eta^2)]}{\sqrt{\sigma^2-\eta^2}}\Psi(\eta)\mathrm{d}\eta = C(\sigma^2,K,\rho\tau), \tag{A-3}$$

with

$$C(\sigma^2,K,\rho\tau) = \pi\left[K+\exp\left\{-\frac{\rho\tau(1+\sigma^2)}{2}\right\}\cdot I_0\left(\frac{\rho\tau[1+\sigma^2]}{2}\right)\right]. \tag{A-4}$$

Equation A-4 can be solved numerically in the following way:[22] First, divide the σ -axis into N equal intervals of $\Delta\sigma$, and transform Eq. A-3 into

$$2\sum_{p=1}^{N}\int_{(p-1)\Delta\sigma}^{p\Delta\sigma}\Psi(\eta)\frac{K+\exp[-\rho\tau\{(N\Delta\sigma)^2-\eta^2\}]}{\sqrt{(N\Delta\sigma)^2-\eta^2}}\mathrm{d}\eta = C((N\Delta\sigma)^2,K,\rho\tau), \tag{A-5}$$

with

$$C((N\Delta\sigma)^2,K,\rho\tau) = \left[K+\exp\left\{-\frac{\rho\tau(1+(N\Delta\sigma)^2)}{2}\right\}\cdot I_0\left(\frac{\rho\tau(1+(N\Delta\sigma)^2)}{2}\right)\right]. \tag{A-6}$$

Next, approximate the function $\Psi(\eta)[K+\exp\{-\rho\tau((N\Delta\sigma)^2-\eta^2\}]$ in the interval $(p-1)\Delta\sigma\leqq\eta\leqq p\Delta\sigma$ by its arithmetic mean

$$\frac{1}{2}\{\Psi(p\Delta\sigma)[K+\exp\{-\rho\tau(N^2-p^2)(\Delta\sigma)^2] + \Psi([p-1]\Delta\sigma)[K+\exp\{-\rho\tau(N^2-[p-1]^2)(\Delta\sigma)^2]\}, \tag{A-7}$$

and perform the integration of the remaining part. Then, we obtain, after some rearrangements,

$$\Psi(\Delta\sigma) = \frac{C((N\Delta\sigma)^2,K,\rho\tau)-\Psi(0)[K+\exp\{-\rho\tau(\Delta\sigma)^2\}]H(1,1)}{(K+1)H(1,1)}, \tag{A-8}$$

$$\Psi(N\Delta\sigma) = \frac{1}{(K+1)H(N,N)}\Big[C((N\Delta\sigma)^2,K,\rho\tau)-\Psi(0)H(N,N)[K+\exp\{-\rho\tau(\Delta\sigma)^2N^2\}]-\sum_{p=1}^{N}\Psi(p\Delta\sigma)[K+\exp\{-\rho\tau(\Delta\sigma)^2(N^2-p^2)\}][H(N,p)+H(N,p-1)\Big], \tag{A-9}$$

with

$$H(N,p) = \sin^{-1}\left(\frac{p}{N}\right) - \sin^{-1}\left(\frac{p-1}{N}\right), \tag{A-10}$$

where

$$\Psi(0) = \frac{1}{K+1}\left[K+\exp\left(-\frac{\rho\tau}{2}\right)\cdot I_0\left(\frac{\rho\tau}{2}\right)\right]. \tag{A-11}$$

The condition A-11 is given by solving the Eq. 9 at $\xi\to0$. Thus, the numerical values of $\Psi(\sigma)$ can be obtained stepwise with $N=1,2,3,\cdots$ for the various choices of the parameters K and $\rho\tau$. Numerical calculations were carried out on a digital computer FACOM M-160 for a series of values of K and $\rho\tau$ ranging from 0 to 100 and 0 to 10, respectively, by setting $\Delta\sigma=0.001$.

References

1) W. M. Schwarz and I. Shain, *J. Phys. Chem.*, **69**, 30 (1965).
2) J. H. Christie, *J. Electroanal. Chem.*, **13**, 79 (1967).
3) J. H. Christie, R. A. Osteryoung, and F. C. Anson, *J. Electroanal. Chem.*, **13**, 236 (1967).
4) R. J. Lawson and J. T. Maley, *Anal. Chem.*, **46**, 559 (1974).
5) K. Holub, *J. Electroanal. Chem.*, **65**, 193 (1975).
6) K. Holub and J. Weber, *J. Electroanal. Chem.*, **73**, 126 (1976).
7) R. C. Bess, S. E. Cranston, and T. H. Ridgway, *Anal. Chem.*, **48**, 1619 (1976).
8) T. H. Ridgway, R. P. Van Duyne, and C. N. Reilly, *J. Electroanal. Chem.*, **67**, 1 (1976).
9) M. K. Hanafey, R. L. Scott, T. H. Ridgway, and C. N. Reilly, *Anal. Chem.*, **50**, 116 (1978) and references therein.
10) S. P. Perone and W. J. Krethow, *Anal. Chem.*, **38**, 1760 (1966).
11) F. C. Anson, *Anal. Chem.*, **38**, 54 (1966).
12) F. C. Anson, J. H. Christie, and R. A. Osteryoung, *J. Electroanal. Chem.*, **13**, 343 (1967).
13) A. Zweig, A. K. Hoffmann, D. L. Maricle, and A. H. Maurer, *J. Am. Chem. Soc.*, **90**, 261 (1968).
14) K. H. Houser, D. E. Bartak, and M. D. Hawley, *J. Am. Chem. Soc.*, **95**, 6033 (1973).
15) E. Temmerman, R. Abel, and R. A. Osteryoung, *J. Electroanal. Chem.*, **55**, 173 (1974).
16) D. L. Jeanmaire and R. P. Van Duyne, *J. Electroanal. Chem.*, **66**, 235 (1975).
17) C. M. Elson, *Inorg. Chem.*, **15**, 469 (1976).
18) J. Weber, K. Holub, D. Homolka and J. Pradac, *J. Electroanal. Chem.*, **73**, 151 (1976).
19) C. J. Myall and D. Pletcher, *J. Electroanal. Chem.*, **75**, 269 (1977).
20) O. G. De Alvarez and L. Gierst, *J. Electroanal. Chem.*, **100**, 819 (1979).
21) H. Matsuda and Y. Ayabe, *Z. Electrochem.*, **59**, 494 (1955).
22) C. Nishihara and H. Matsuda, *J. Electroanal. Chem.*, **51**, 287 (1974).
23) Y. Fujii, E. Kyuno, and R. Tsuchiya, *Bull. Chem. Soc. Jpn.*, **43**, 786 (1970).
24) T. Ohsaka, N. Oyama, S. Yamaguchi, and H. Matsuda, *Bull. Chem. Soc. Jpn.*, **54**, 2475 (1981).
25) N. Oyama and H. Matsuda, *J. Electroanal. Chem.*, **78**, 89 (1977).
26) T. Rohko, M. Kogoma, and S. Aoyagui, *J. Electroanal. Chem.*, **78**, 89 (1977).
27) T. Ohsaka, N. Oyama, and H. Matsuda, *Bull. Chem. Soc. Jpn.*, **53**, 3601 (1980).
28) J. P. Jones and D. W. Margerum, *J. Am. Chem. Soc.*, **92**, 470 (1970).
29) J. H. Baxendale and P. George, *Trans. Faraday Soc.*, **46**,

736 (1950).
30) J. Burgess and M. V. Twigg, *J. Chem. Soc., Dalton Trans.*, **1974**, 2032.
31) N. Shinohara, J. Lilie, and M. G. Simic, *Inorg. Chem.*, **16**, 2809 (1976).
32) J. Lilie, N. Shinohara, and M. G. Simic, *J. Am. Chem. Soc.*, **98**, 6516 (1976).
33) M. G. Simic, M. Z. Hoffman, R. P. Cheney, and Q. G. Mulazzani, *J. Phys. Chem.*, **83**, 439 (1979).
34) R. Farina, R. Hogg, and R. G. Wilkins, *Inorg. Chem.*, **7**, 170 (1968).
35) R. Davies, M. Green, and A. G. Sykes, *J. Chem. Soc. Dalton Trans.*, **1972**, 1171.
36) D. Meisel, K. H. Schmidt, and D. Meyerstein, *Inorg. Chem.*, **18**, 971 (1979).
37) M. Kodama, Y. Fujii, and T. Ueda, *Bull. Chem. Soc. Jpn.* **43**, 2085 (1970).
38) M. Kodama, M. Hashimoto, and T. Watanabe, *Bull. Chem. Soc. Jpn.*, **45**, 2761 (1972).
39) G. G. Hammes and J. I. Steinfeld, *J. Am. Chem. Soc.*, **84**, 4639 (1962).
40) K. Kustin, R. F. Pasternack, and E. M. Weinstock, *J. Am. Chem. Soc.*, **88**, 4610 (1966).
41) A. Kowalak, K. Kustin, R. F. Pasternack, and S. Petrucci, *J. Am. Chem. Soc.*, **89**, 3126 (1967).
42) A. K. S. Ahmed and R. G. Wilkins, *J. Chem. Soc.*, **1960**, 2901.
43) R. F. Pasternack, M. Angwin, L. Gippand, and R. Reingold, *J. Inorg. Nucl. Chem.*, **34**, 2329 (1972).
44) R. G. Wilkins, *J. Chem. Soc.*, **1957**, 4521.
45) R. Hogg and R. G. Wilkins, *J. Chem. Soc.*, **1962**, 341.
46) "Coordination Chemistry," ed by A. E. Martell, American Chemical Society, Washington, D. C. (1978), Vol. 2, p. 85.